Journal of the European Ceramic Society 21 (2001) 2903–2910

www.elsevier.com/locate/jeurceramsoc

Estimation of the phase diagram for the ZrO_2–Y_2O_3–CeO_2 system

L. Li [a], O. Van Der Biest [b,*], P.L. Wang [c], J. Vleugels [b], W.W. Chen [c], S.G. Huang [a]

[a] *Department of Materials Science and Engineering, Shanghai University, 200072 Shanghai, China*
[b] *Department of Metallurgy and Materials, Katholike Univerteit Leuven, B-3001 Leuven, Belgium*
[c] *The State Key Lab of High Performance Ceramics and Superfine Microstructure, Shanghai Institute of Ceramics, Chinese Academy of Science, 200050 Shanghai, China*

Received 22 November 2000; accepted 20 January 2001

Abstract

Comprehensive descriptions of the thermodynamic properties and experimental information in three oxide systems ZrO_2–Y_2O_3, ZrO_2–CeO_2 and Y_2O_3–CeO_2 are given and thermodynamic models for the calculation of these systems are discussed. The phase diagrams of the quasi-ternary ZrO_2–Y_2O_3–CeO_2 system in the zirconia-rich corner are estimated at different temperatures with a substitutional model and Muggianu's extrapolation. The equilibrium phase diagram calculation is extended to low temperatures, as well as the Gibbs free energy of the tetragonal, monoclinic and cubic phases of zirconia doped with yttria and ceria.

Keywords: CeO_2; Phase equilibria; Thermodynamic calculation; Y_2O_3; ZrO_2

1. Introduction

ZrO_2-containing ceramics are of great importance in many applications such as high temperature electrolytes in fuel cells, magnetohydrodynamic electrodes, oxygen gas sensors, heat-resistant linings of high temperature furnaces, biomaterials, and others.[1,2] Besides, due to the stress induced martensite transformation occurring in this material, through which the metastable tetragonal phase can spontaneously transform to the monoclinic phase, an associated shape memory effect might yield another tremendous potential for applications of this material. Moreover, ZrO_2-containing ceramics also find their way to applications in the engineering field. As known, Y_2O_3 doping of ZrO_2 results in a material with very high toughness and strength, and acceptable hardness. Doping of ZrO_2 with CeO_2 even results in tougher materials, but the hardness is not high enough to be used for wear applications. In order to document the effect of combined CeO_2 and Y_2O_3 doping of ZrO_2 ceramics, this work aims to estimate the phase diagrams of ZrO_2–Y_2O_3–CeO_2 system and the Gibbs free energy of phases in the ZrO_2-rich corner at different temperatures, based on the knowledge of the limiting quasi-binary systems so as to offer suggestions for further development and potential applications.

2. Experimental information and previous assessments of the limiting quasi-binaries

There have been a lot of experimental determinations of phase equilibria in the ZrO_2-containing systems especially in the quasi-binaries of ZrO_2–Y_2O_3 and ZrO_2–CeO_2. Early work may be recalled from the 1950s which was contributed by Duwez et al.[3,4] However, because of the sluggish reaction kinetics, the formation of metastable phases during long time sintering, the difficulties in conducting experiments at high temperatures, there was no general agreement between the early and recent works. Much research has been done in ZrO_2-containing systems since 1960. Rouanet,[5] found that the liquidus temperature rose slightly as the yttria content increased, reaching a rather flat maximum at about 37.4 mol%

* Corresponding author. Tel.: +32-16-321-264; fax: +32-16-321-992.
E-mail address: omer.vanderbiest@mtm.kuleuven.ac.be (O. Van Der Biest).

0955-2219/01/$ - see front matter
PII: S0955-2219(01)00218-7

$YO_{1.5}$ and 2800°C, and then fell to the eutectic point. Stubican et al.[6] determined again part of the liquidus in the yttria rich corner and found their results agreed well with that of Rouanet,[5] but suggested a peritectic reaction in the system. Noguchi et al.[7] determined the liquidus which was lower than that of Rouanet.[5] Since it was very difficult to identify the liquidus from these experimental results, Du et al.[8,39] used two sets of liquidus data. One from Rouanet[5] together with data of Stubican[6] at the high temperatures. The other was from Noguchi et al.[7] For convenience, the optimised results will be designated here as set A and set B, respectively.

Besides, the stoichiometric phase $Y_2Zr_2O_7$, postulated by Rouanet[9] was not found by others. Ray[10] showed afterwards that long time annealing of a $2ZrO_2Y_2O_3$ mixture did not yield the ordered pyrochlore compound. However, the hexagonal $Y_4Zr_3O_{12}$ compound was found, which decomposed above 1250°C. This result agreed well with other work and was accepted in the optimisation of Du et al.[8]

Early conflicts concerned the existence of a distinct two-phase region (fcc solid solution + bcc solid solution) or whether the structures of these phases were essentially the same. In the optimisation,[8,39] only the single phase was considered.

The solubility of Y_2O_3 in tetragonal ZrO_2 in the ZrO_2-rich portion was firstly measured by Srivastava et al.[11] and their work matched well with many other measurements. Ruh et al.[12] reported smaller values, but Pascual[13] published larger ones. Therefore, the solubility data in Refs. 12 and 13 were not used in the optimisation of Du et al.[8,39] The calculated ZrO_2–$YO_{1.5}$ phase diagram with data set B of Du et al.[8] is shown in Fig. 1. In order to save space, the tetragonal, monoclinic and cubic solid solutions are abbreviated as tss, mss and css, respectively. The $YO_{1.5}$, ZrO_2 and CeO_2 components are abbreviated as YO, ZO and CE. Some experimental results, on which the authors relied heavily during the calculation are plotted on the diagram. It is found that though the system is rather complicated and there exist miscellaneous reports about the solubility limits and phase boundaries, the optimised result is still satisfactory in comparison with the experimental results.

The original optimisation[8,39] was performed with the help of the Lukas program; in the present work, the calculated parameters have been transferred into Thermo-Calc software format since the estimation of the quasi-ternary system was performed using this software.

Apparent discrepancies occurred in previous reports in the ZrO_2–CeO_2 system, especially in the high temperature ZrO_2-rich solid solution region as well as on the possible low temperature ordering phenomena. Using precision lattice parameter measurements for the investigation of high temperature phase boundaries and DTA for the low temperature phase region and eutectoid reaction, Duran et al.[14] reported that in the high temperature range there existed two phases as Fss (fcc solid solution) + Css (cubic solid solution) extending from 18 mol%. They suggested the existence of a eutectic at 2300°C and 24 mol% CeO_2. Besides, they also confirmed the existence of the $Ce_2Zr_3O_{10}$ compound in the low temperature range, which met well with the results of Longo.[15] However, Ramesh et al.[16] reported they found no evidence of the metastable phase $Ce_2Zr_3O_{10}$ after microwave sintering of ZrO_2–CeO_2 at 1500°C. Yashima et al.[17] pointed out that earlier work did not take into account the fact that the Ce^{+4} ion partially reduced to Ce^{+3} at about 1400°C so that the high temperature portion of the ZrO_2–CeO_2 phase diagram determined by experiments was actually that of $(Zr,Ce^{+4}, Ce^{+3})O_{2-x}$.They labelled this part of the diagram as "defective". These authors also discussed the possibility of the

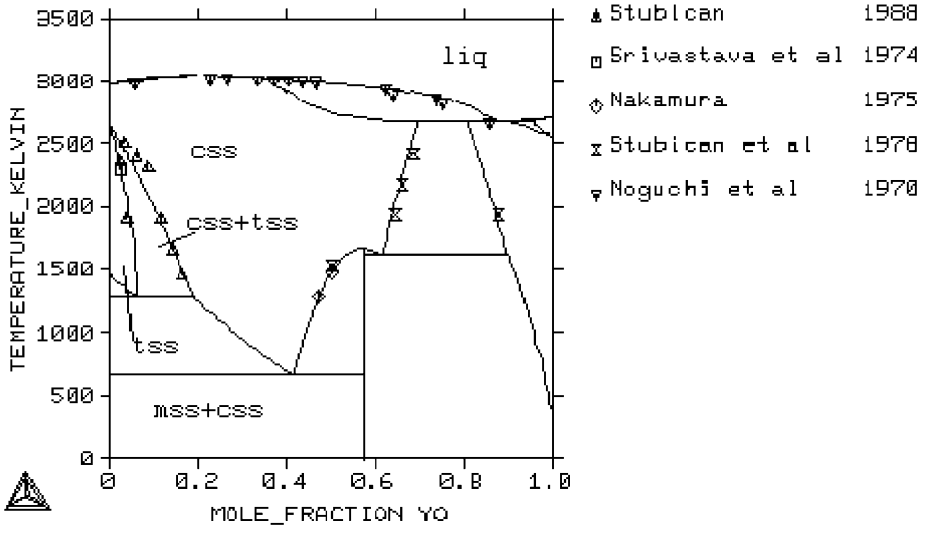

Fig. 1. Calculated and experimental results[8,39] of the ZrO_2–$YO_{1.5}$ system.

existence of the ordering phase $Ce_2Zr_3O_{10}$, which they did not confirm but explained that the confusion about the existence was caused by a cation-diffusionless phase transformation producing the metastable t′ phase.

A thermodynamic evaluation of the ZrO_2–CeO_2 system was contributed by Du et al.[18,40] These authors made an extensive literature search and put many of the experimental results into optimisation. They produced optimised phase diagrams and also the T_0 lines, i.e. the temperature where the Gibbs free energies of the tss and mss are equal

In order to give a clear description of the system, especially below 1400°C, Tani et al.[19] argued that these discrepancies might be caused by the extremely sluggishness of the cation diffusion in comparison with the oxygen diffusion and an equilibrium state could not be obtained by normal heat treating procedures even after long time annealing. Those authors[20] accelerated the reaction velocity at low temperatures under hydrothermal conditions and pointed out that the influences of such treatment only affected the kinetics of the reaction but had no effect on the characteristics of the final products. These authors thus established the phase diagram of this system again through careful work to obtain not only the solubilities of phases at low temperatures but also the stability of the stoichiometric phase. Based on the experimental work of Refs.19 and 20, one of the present authors[21,41] evaluated the ZrO_2–CeO_2 system thermodynamically with the subregular model. Lattice stability parameters of ZrO_2 of liquid, cubic, tetragonal and monoclinic phases were taken from Du et al.[8,39] In order to give a good description of the thermodynamic properties of the tetragonal and monoclinic phase which are very important for applications, the tss and mss phase boundaries were carefully fitted[21,41] with the Lukas program.[22] As plotted in Fig. 2, there still exist differences between the calculated and experimental

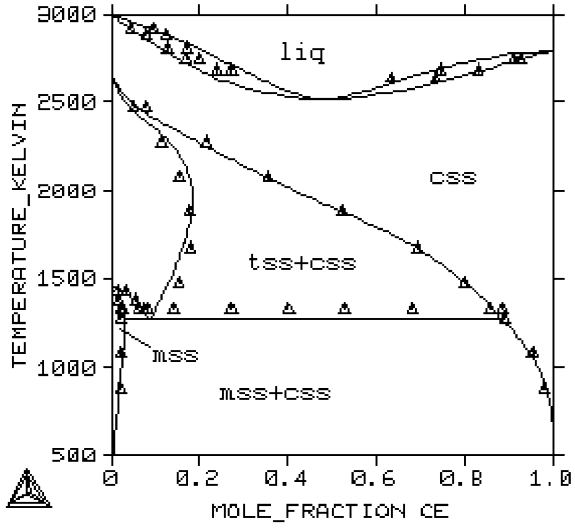

Fig. 2. Calculated and experimental results[19] of the ZrO_2–CeO_2 system.

eutectoid temperature. However, if this line is fitted very well, the boundary of mss and tss phases can not be optimised satisfactorily. Considering the importance of these phases and taking into account the measurement error on the eutectoid temperature, which was about 50°C,[19] the authors[21,41] preferred to maintain the results as shown in Fig. 2. The calculated result was transferred into Thermo-Calc format for the same reason as stated above and shown in Fig. 2. together with the experimental results of Tani.[19] The optimised solution coefficients and lattice stability parameters were used to calculate the T_0 temperature and martensite transformation temperature M_s[23,24] as well.

The available experimental information on the Y_2O_3–CeO_2 quasi-binary is very limited. Longo and Podda[25,26] used CeO_2 (99.9% pure) and Y_2O_3 (99.99% pure) to prepare stoichiometric mixtures, which were homogenised in an agate mortar for 4 h, pressed and pre-heated at 1400°C for 500 h. After these treatments, the specimens were re-fired at different temperatures for times long enough to ensure the attainment of true equilibrium conditions. In every case, they checked the completion of the reaction and considered the reactions to be completed only when successive microscopic observations revealed no variations in the number and proportions of the phases present and the intensities of diffraction lines remained unchanged in successive X-ray diffraction pattern measurements. They froze the phase relations at high temperatures through air quenching. They confirmed that there was no compound formed under the operation, but there existed two extensive solid solutions. The solubility limit of the css and yss solid solution phases at various temperatures were determined by accurate measurement of the lattice parameters. They argued that this measurement was valid since the variation of the lattice parameters of two solutions was just a function of composition and agreed well with Vegard's Law; the slopes of the lines at various temperatures also coincided well. However, in spite of the early statement of the existence of two phases,[25,26] some of the present authors[27] estimated the thermodynamic properties of the css(yss) phase by treating them as a miscibility gap according to the detected solubility limits of CeO_2 in yss and $YO_{1.5}$ in css in the Y_2O_3–CeO_2 system.[25,26] This consideration maintained consistent with the previous work.[8,39] The calculated phase field and the measured solubility limits[25,26] are shown in Fig. 3. Ref. 27 also extended the css + yss phase region into the ZrO_2–Y_2O_3–CeO_2 system using the Bonnier equation and this agreed well with the experimental results.

3. Thermodynamic model

Thermodynamic modelling of oxide systems sometimes becomes complicated. As temperature increases,

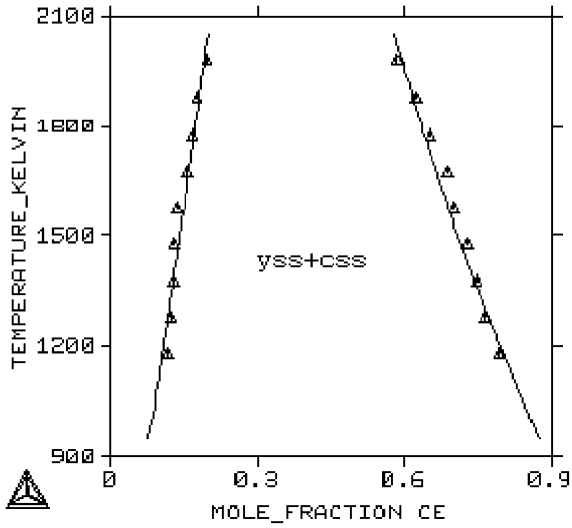

Fig. 3. Calculated and experimental results[25,26] of the $YO_{1.5}$–CeO_2 system.

the well-ordered arrangements of the crystal lattice might break down. When long range order disappears, short range order could still exist but decreases at higher temperatures. It is also possible in oxide systems that there exist different tendencies of chemical ordering according to the kind of ions present. In the molten state, there might exist molecular-like associations between unlike atoms.[28] In order to give a better description of such situation, Hillert and Staffansson[29] developed a two-sublattice model suggesting vacancy at one of the sublattices. Afterwards, Fernandez Guillermet et al.[30] introduced vacancies at both sublattices, which might fit the requirements of structure and electro-neutrality. However, in the case of the liquid phase without molecular-like associates or in the case of crystalline phases without shortage of elements in sublattices, the problem in oxides become easier. Kaufman and Nessor[31] contributed firstly a substitutional model which considered an oxide as one pure component in the formalism of the Gibbs free energy of phases, If none of the complications mentioned above arise, this model has been applied successfully to many oxide systems by some of the present authors.[32–34] The present authors also demonstrated that in the case stated above, the substitutional model is represented by exactly the same mathematical formalism as the sublattice model, when the valence of the cations remained the same.[35]

For the ZrO_2–Y_2O_3–CeO_2 system, there are several reports concerning the lattice structure.[36–38] Esquivias et al.[36] prepared zirconia–yttria solid solutions through controlled hydrolysis of alkoxides, and found by X-ray absorption spectroscopy (XAS) measurements that Y atoms were in the ZrO_2 lattice from the very beginning of the process and exhibited some short-range order. With the dark field image technique and the measurement of diffraction patterns of the phases, Lelait et al.[37] found that there was one $(Zr,Y)O_2$ group on each lattice point in the cubic FCC lattice and two such groups in the C-face centered tetragonal lattice. However, the authors did not explain how to fit the requirements of electrical neutrality during the change of position of cations. Kondoh et al.[38] pointed out that when ZrO_2 is doped with Y_2O_3, the solid solution is formed by substituting Y^{+3} for Zr^{+4} and forming O^{-2} vacancies so as to maintain electrical neutrality. Through XAS study, these authors showed a decrease in the first neighbour coordination number of Zr ions implying the occurrence of short range order of oxygen ion and vacancies. These descriptions showed some aspects about the physical structures. However, it is still not enough to give a clear image of the structures, which could be used to account for the mixing with the sublattice model. In order to estimate ternary diagrams of this system, the substitutional model has still been applied in the present work, where the Gibbs free energy of one mole solution phase in the structure ϕ in the binary system is written as:

$$G_m^{\Phi}(x,T) = \sum_{i=1}^{2} x_i {}^{o}G_i^{\Phi}(T) + RT\sum x_i \ln x_i + x_1 x_2 \sum_{j=0}^{1} k_{(j+3)}(x_1 - x_2)^j \quad (1)$$

In Eq. (1), the first summation is the mechanical mixture of the pure components, the second refers to the ideal solution, and the third to the Gibbs excess energy, which is in the format of a Redlich–Kister polynomial. K_j in Eq. (1) can be expressed as:

$$K_j = A_j + B_j T + C_j T \ln T + D_j T^2 + E_j/T + F_j T^3 \quad (2)$$

The Gibbs free energy of a ternary solution phase has been obtained through the extrapolation from the binary solution phases on the basis of Muggianu's equation. According to this equation and in a subregular solution model, the last term in Eq. (1) expands to:

$$G_{mix}^{xs} = x_A x_B\left\langle L_{AB}^0 + L_{AB}^1(x_A - x_B)\right\rangle + x_B x_C\left\langle L_{BC}^0 + L_{BC}^1(x_B - x_C)\right\rangle + x_A x_C\left\langle L_{AC}^0 + L_{AC}^1(x_A - x_C)\right\rangle \quad (3)$$

Other widely used geometric methods, such as the equations of Kohler has also been used to estimate the ternary system in the present work. However, Muggianu's equation is found to give the best fitting of the experimental information in the present system.

4. Estimation of the quasi-ternary system

Lattice stability parameters for ZrO_2, Y_2O_3 and CeO_2 were taken from Du et al.[6] and Li et al.[19] and are listed in Table 1, where l-ZrO_2, c-ZrO_2, t-ZrO_2, m-ZrO_2 referred to the liquid, cubic, tetragonal and monoclinic phases of zirconia, respectively. Model parameters for ZrO_2–Y_2O_3,[8,39] ZrO_2–CeO_2[21] and Y_2O_3-CeO_2.[27] Quasi-binaries are listed in Table 2. Moreover, there do not exist any metastable tss and mss phases in the Y_2O_3–CeO_2 system, these occur as limited phase regions in the ZrO_2–Y_2O_3 and ZrO_2–CeO_2 systems at the high ZrO_2 content corner. Thus the model parameters for these metastable phases in the Y_2O_3–CeO_2 system were assumed to be big numbers and put into the calculation. These parameters were combined together to estimate the phase diagrams at zirconia-rich corner. It should also be mentioned that there exist two sets of solution parameters in the ZrO_2-Y_2O_3[8,39] system, however only data set B has been adopted in the present work. The thermodynamic calculation of the zirconia-rich corner of the ternary system was conducted by Thermo-Calc software.

The predicted ternary phase diagrams of the zirconia-rich corner at different temperatures are shown in Fig. 4(a)–(g). Tie lines are also shown in Fig. 4(a)–(d). The Gibbs free energies, as functions of temperature, of mss, css and tss phases were also calculated and are shown in Fig. 5. for a material with composition: 10.0 mol% CeO_2, 1.0 mol% $YO_{1.5}$ and 89.0 mol% ZrO_2.

In order to check the calculated phase diagrams, the present authors prepared three samples with the composition listed in Table 3. The powder mixtures were ground in pure ethanol for 24 h by planetary ball milling in a plastic bottle and then dried. Compacted pellets of dried powder were dry-pressed and subsequently heated in air at 1300°C for different times. Phase identification was performed by X-ray diffraction (XRD) in a Guinier-Hagg camera with CuK_{α_1} radiation and Si as an internal standard. Annealing experiments were performed until consecutive X-ray diffraction analysis of the heated samples revealed no further variations in the number of phases and the intensities of the diffraction lines. After

Table 1
Summary of lattice stability parameters (units in J/mol of cation)

${}^oG^{l-ZrO_2} = 0.0$	${}^oG^{t-ZrO_{1.5}} = -35617.50 + 26.46250T$
${}^oG^{c-ZrO_2} = -87986.6 + 29.49600T$	${}^oG^{m-YO_{1.5}} = -14697.50 + 29.91500T$
${}^oG^{t-ZrO} = -93954.8 + 31.75500T$	${}^oG^{l-CeO_2} = 0.0$
${}^oG^{m-ZrO_2} = -99978.8 + 35.89800T$	${}^oG^{c-CeO_2} = -195800.00 + 70.018T$
${}^oG^{l-YO_{1.5}} = 0.0$	${}^oG^{t-CeO_2} = -87917.50 + 39.783T$
${}^oG^{c-YO_{1.5}} = 67419.30 + 25.10500T$	${}^oG^{m-CeO_2} = -11697.50 + 288.915T$

Table 3
Starting compositions and identified phases of the ceramic samples

Ceramic	ZrO_2 mol%	Y_2O_3 mol%	CeO_2 mol%	Phases
1	0.313	0.053	0.634	css + tss
2	0.277	0.077	0.646	css
3	0.444	0.112	0.444	css + tss

Table 2
Summary of the solution parameters used in this work

Phase	Reference state		K_3 (J/mol of cation)	K_4 (J/mol of cation)
ZrO_2–$YO_{1.5}$ system				
Liquid	Liquid ZrO_2	Liquid $YO_{1.5}$	−183750.80 + 72.39814T	−48733.30 + 9.47562T
css (yss)	c-ZrO_2	c-$YO_{1.5}$	−12059.50 + 11.15647T	−13783.50-5.37868T
hss	c-ZrO_2	h-$YO_{1.5}$	50419.50	
tss	t-ZrO_2	t-$YO_{1.5}$	−25800.20	
mss	m-ZrO_2	m-$YO_{1.5}$	−58222.90 + 98.12601T	

$\Delta G1/7Zr_3Y_4O_{12} = 37^0G^{c-ZrO_2} + 4/7^0G^{c-YO_{1.5}} - 3284.3 - 2.26749T$

ZrO_2–CeO_2 system				
Liquid	Liquid ZrO_2	Liquid $YO_{1.5}$	−243651.45 + 58.96182T	123981.04-47.84299T
css (yss)	c-ZrO_2	c-CeO_2	108583.50-54.62258T	60175.77-24.91597T
tss	t-ZrO_2	t-CeO_2	−54284.36	
mss	m-ZrO_2	m-CeO_2	−146064.78-238.20385T	
$YO_{1.5}$–CeO_2 system				
css (yss)	c-$YO_{1.5}$	c-CeO_2	11168.97 + 11.00000T	−2852.630 + 4.78084T
tss	t-ZrO_2	t-CeO_2	240T	
mss	m-ZrO_2	m-CeO_2	400T	

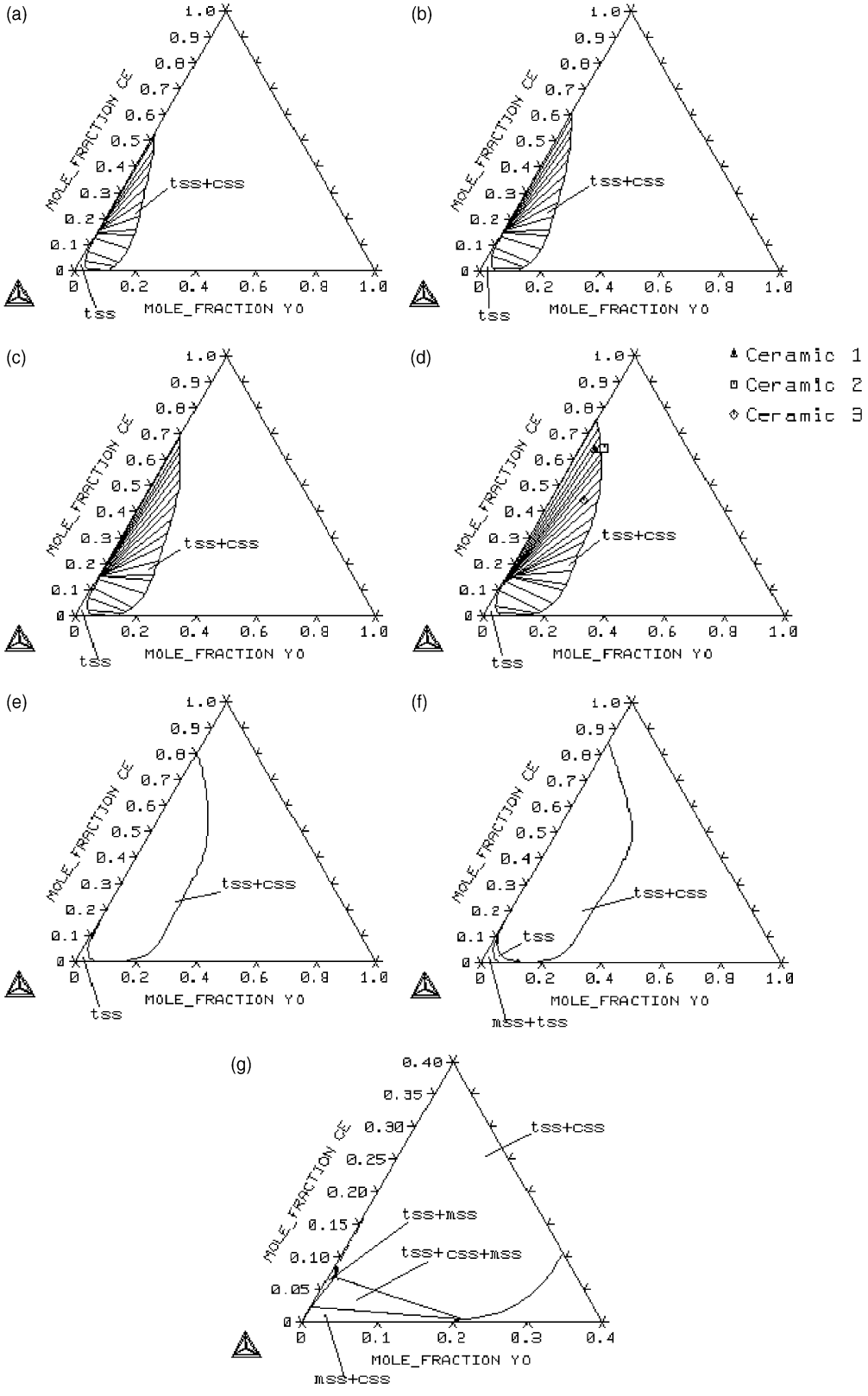

Fig. 4. Phase diagram of the zirconia-rich corner in the ZrO_2–$YO_{1.5}$–CeO_2 system at (a) 1600°C; (b) 1500°C; (c) 1400°C; (d) 1300°C; (e) 1200°C; (f) 1100°C; (g) 1000°C.

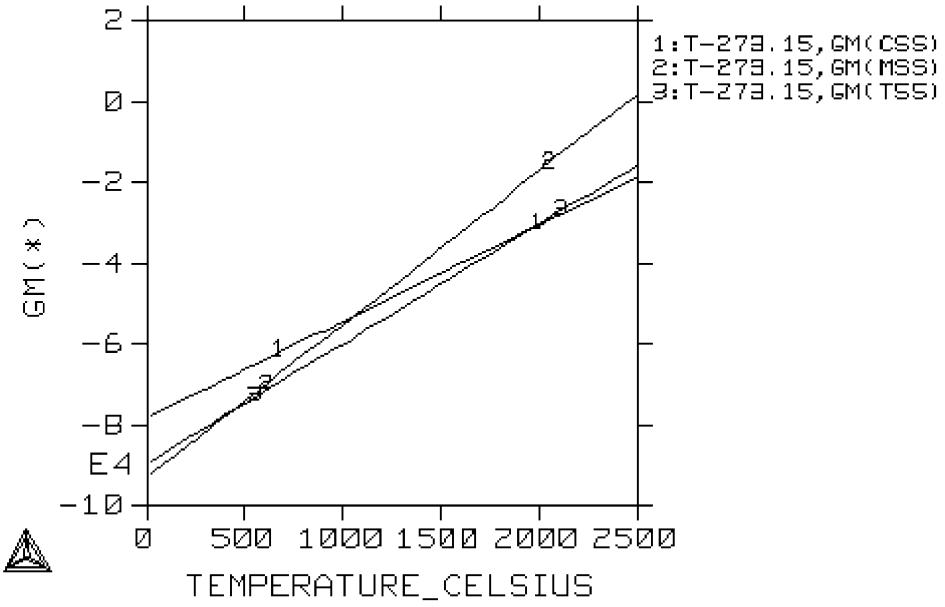

Fig. 5. Gibbs free energies of the mss, css and tss phases, where GM(*) is in J/mol of cation.

annealing for 250 h, ceramic 2 was only composed of the css phase, whereas ceramics 1 and 3 were mainly constituted of css with a minor amount of tss solid solution. These experimental results agree very well with the calculated results, as shown in Fig. 4(d).

The equilibrium phase diagrams were also calculated at lower temperatures. At 1000°C, there is a three-phase region composed of tss, css and mss phases. On the ZrO_2-rich side of this field there is a two-phase region of mss + css with single phase mss and css setting at both sides of the two-phase field. A narrow two-phase region of tss + mss was present, adjacent to the three-phase field. A single-phase tss region also exists but it is so small that it appears only as a thick line in the diagram plotted in Fig. 4(g). All these features agree well with the information from the limiting quasi-binaries, either calculated or measured.

From Fig. 5., one can obtain the T_0 temperature, i.e. the temperature at which the Gibbs free energies of two different phases were equal. This information might be useful for the study of phase transformation and the preparation of samples in this system.

5. Summary

The phase diagrams in the zirconia-rich corner of the quasi-ternary ZrO_2–Y_2O_3–CeO_2 system in the temperature region between 1000 and 1600°C have been estimated based on the comprehensive knowledge of the thermodynamic properties of the limiting quasi-binaries. Experimental verification has been also performed showing that the estimated phase diagrams are reliable. Equilibrium phase diagrams at lower temperatures are consistent with the available experimental data and previously calculated information.

Acknowledgements

This work is financially supported by the Flanders-China bilateral project (BIL 99/10). The authors are thankful to Professor H.L. Lukas for offering the new version of the Lukas Program.

References

1. Piconi, C. and Maccauro, G., Zirconia as a ceramic biomaterial. *Biomaterials*, 1999, **20**, 1–25.
2. Hannink, R. H. J., Kelly, P. M. and Muddle, B. C., Transformation toughening in zirconia-containing ceramics. *J. Am. Ceram. Soc.*, 2000, **83**(3), 461–487.
3. Duwez, P., Brown, F. H. and Odeli, F., The zirconia-yttria system. *J. Electrochem. Soc.*, 1951, **98**(9), 356–362.
4. Duwez, P. and Odeli, F., Phase relationships in the system zirconia–ceria. *J. Am. Ceram. Soc.*, 1950, **33**, 274.
5. Rouanet, A., High temperature solidification and phase diagrams of the ZrO_2–Er_2O_3, ZrO_2–Y_2O_3 and ZrO_2–Yb_2O_3 systems. *C. R. Seances Acad. Sci., Ser. C*, 1968, **267**(23), 1581–1584.
6. Stubican, V. S., Hink, R. C. and Ray, S. P., Phase equilibria and ordering in the system ZrO_2–Y_2O_3. *J. Am. Ceram. Soc.*, 1978, **61**(1–2), 17–21.
7. Noguchi, T., Mizuno, M. and Yamada, T., The liquidus curve of the ZrO_2–Y_2O_3 system as measured by a solar furnace. *Bull. Chem. Soc. Jpn.*, 1970, **43**(8), 2614–2616.
8. Du, Y., Jin, Z. P. and Huang, P. Y., Thermodynamic assessment of the ZrO_2–$YO_{1.5}$ system. *J. Am. Ceram. Soc.*, 1991, **74**(7), 1569–1577.
9. Rouanet, A., Contribution a l'etude des systemes zircone-oxides des lanthanides au voisinage de la fusion. *Rev. Int. Hautes Temp. Refract*, 1971, **8**(2), 161–180.

10. Ray, S. P. and Stubican, V. S., Fluorite related ordered compounds in the ZrO_2–CaO and ZrO_2–Y_2O_3 system. *Mater. Res. Bull.*, 1977, **12**(5), 549–556.
11. Srivastava, K. K., Patil, R. N., Choudhary, C. B., Gokhale, K. V. G. K. and Stubarao, E. C., Revised phase diagram of the system of ZrO_2–$YO_{1.5}$. *Trans. J. Br. Ceram. Soc.*, 1974, **73**(2), 85–91.
12. Ruh, R., Mazdiyasni, K. S., Valentine, P. G. and Bielstein, H. O., Phase relations in the system ZrO_2–Y_2O_3 at low Y_2O_3 contents. *J. Am. Ceram. Soc.*, 1984, **67**(9), C-190–C-192.
13. Pascual, C. and Duran, P., Subsolidus phase equilibria and ordering in the system ZrO_2–Y_2O_3. *J. Am. Ceram. Soc.*, 1983, **66**(1), 23–27.
14. Duran, P., Gonzalez, M., Moure, C., Jurado, J. R. and Pascual, C., A new tentative phase equilibrium diagram for the ZrO_2–CeO_2 sysem in air. *J. Mater. Sci.*, 1990, **25**(12), 5001–5006.
15. Longo, V. and Minichelli, D., X-ray characterization of $Ce_2Zr_3O_{10}$. *J. Am. Ceram. Soc.*, 1973, **56**(11), 600.
16. Ramesh, P. D., Sarin, P., Jeevan, S. and Rao, K. J., *J. Mater. Synth. Process*, 1996, **4**(3), 163–173.
17. Yashima, M., Takshina, H., Kakihana, M. and Yoshimura, M., Low-temperature phase equilibria by the flux method and the metastable-stable phase diagram in the ZrO_2–CeO_2 system. *J. Am. Ceram. Soc.*, 1994, **77**(7), 1869–1874.
18. Du, Y., Yashima, M., Koura, T., Kakihana, M. and Yoshimura, M., Thermodynamic evalution of the ZrO_2–CeO_2 system. *Scripta Metall. Mater.*, 1994, **31**(3), 327–332.
19. Tani, E., Yoshimura, M. and Somiya, S., Revised phase diagram of the system ZrO_2–CeO_2. *J. Am. Ceram. Soc.*, 1983, **66**, 506–520.
20. Tani, E., Yoshimura, M. and Somiya, S., Effect of mineralizers on the crystallization of the solid solutions in the system ZrO_2–CeO_2 under hydrothermal conditions. *Yogvo-Kyokai Shi*, 1982, **90**(4), 195–201.
21. Li, L., Xu, Z. Y. and Ao, Q., Optimization of the phase diagram of CeO_2–ZrO_2 system. *J. Mater. Sci. Technol.*, 1996, **12**, 159–160.
22. Lukas, H. L., Hening, E.Th. and Zimmermann, B., Optimization of phase diagrams by a least squares method using simultaneously different types of data. *CALPHAD*, 1977, **1**, 225–236.
23. Xu, Z. Y., Li, L. and Jang, B. H., Thermodynamic calculation of the equilibrium temperature between the tetragonal and monoclinic phases in CeO_2–ZrO_2. *Mater Trans. JIM*, 1996, **37**(6), 1281–1283.
24. Jang, B. H., Li, L. and Xu, Z. Y., Thermodynamic calculation of the M_s temperature in 8 mol% CeO_2–ZrO_2. *Mater Trans. JIM*, 1996, **37**(6), 1284–1286.
25. Longo, V. and Podda, L., Phase equilibrium diagram of the system ceria-yttria for temperatures between 900 and 1700°C. *J. Mater. Sci.*, 1981, **16**(3), 839–841.
26. Longo, V. and Podda, L., Relazioi tra le fasi allo stato solido nel sistema CeO_2–ZrO_2–Y_2O_3 tra 1700 e 1400 °C. *Ceramica (Florence)*, 1984, **37**(5), 18–20.
27. Huang, S. G., Li, L., Van Der Biest, O. and Wang, P. L., Estimation of the phase diagram in ZrO_2–$YO_{1.5}$–CeO_2 system. *J. Shanghai University*, 2000, **6**(4), 189–192 (in Chinese)..
28. Jordan, A. S. In Y. A. Chang, and J. F. Smith ed. *Calculation of Phase Diagram and Thermochemistry of Alloy Phases*, TMS-AIME, 1979.
29. Hillert, M. and Staffansson, L.-I., An analysis of the phase equilibria in the Fe–FeS system. *Metall. Trans.*, 1975, **6B**, 37–41.
30. Fernandes Guillermet, A., Hillert, M., Jasson, B. and Sundman, B., An assessment of the Fe–S system using a two-sublattice model for the liquid phase. *Metall. Trans.*, 1981, **12B**, 745–754.
31. Kaufman, L. and Nesor, H., Calculation of quasibinary and quasiternary oxide systems-I. *CALPHAD*, 1978, **2**, 35–53.
32. Li, L., Sun, W. Y., Wang, P. L. and Tang, Z. J., The calculation of phase diagrams of Al_2O_3–SiO_2–R_2O_3 systems. *Phys. Chem. Glasses*, 1997, **38**(6), 323–326.
33. Li, L., Tang, Z. J., Sun, W. Y. and Wang, P. L., Phase diagram estimation of Al_2O_3–SiO_2–Gd_2O_3 systems. *Phys. Chem. Glasses*, 1999, **40**(3), 126–129.
34. Li, L., Tang, Z. J., Sun, W. Y. and Wang, P. L., Phase diagram estimation of Al_2O_3–SiO_2–La_2O_3 systems. *J. Mater Science and Technology*, 1999, **15**(4), 439–442.
35. Li, L., Van Der Biest, O., Wang, P. L. and Sun, W. Y., Application of substitutional model in oxide systems. *CALPHAD,* submitted.
36. Esquivias, L., Barrera-Solano, C., Pinero, M. and Prieto, C., Short-range order of yttria doped zirconia powders studied by X-ray absorption (II). *J. Alloys and Compounds*, 1996, **239**, 71–76.
37. Lelait, L. and Alperine, S., T.E.M. investigations of high toughness non-equlibrium phases in the ZrO_2–Y_2O_3 system. *Scripta Metall. Mater.*, 1991, **25**(8), 1815–1820.
38. Kondoh, J., Kikuchi, S., Tomii, Y. and Ito, Y., Effect of aging on yttria-stabilized zirconia. *J. Electrochem. Soc.*, 1998, **145**(5), 1550–1560.
39. Ondik, H. M. and Mcmurdie, H. F. (eds), *Phase Diagrams for Zirconium + Zirconia Systems*. Am. Ceram. Soc. OH, 1998, p. 114.
40. Ondik, H. M. and Mcmurdie, H. F. (eds), *Phase Diagrams for Zirconium + Zirconia Systems*. Am. Ceram. Soc., OH, 1998, p. 126.
41. Ondik, H. M. and Mcmurdie, H. F. (eds), *Phase Diagrams for Zirconium + Zirconia Systems*. Am. Ceram. Soc. OH, 1998, p. 123.